Atmospheric correction of satellite data using aerosol information derived from multi-wavelength lidar observation

Mitsuo Minomura, Jianfei Ru, Hiroaki Kuze, and Nobuo Takeuchi
Center for Environmental Remote Sensing(CEReS),
Chiba University, 1-33, Yayoi-cho, Inage-ku, Chiba, 263 Japan
mino@rsirc.cr.chiba-u.ac.jp

January 22, 1998

1 Introduction

The radiative transfer codes, for example MODTRAN3, employ the standard atmospheric models. However the actual conditions of atmosphere, especially those of aerosol particles, change both spatially and temporally. It is highly desirable to make use of the relevant data measured simultaneously to perform the atmospheric correction on the satellite data.

The lidars are quite useful to obtain aerosol information under in-situ conditions. A multi-wavelength lidar system (1064, 756, 532, and 355 nm) was constructed at the Center for Environmental Remote Sensing (CEReS), Chiba University in March, 1996 and it has been applied to the atmospheric correction of satellite data.

We compare the results obtained with aerosol profiles based on the multi-wavelength lidar measurements and those obtained by using the standard atmospheric models.

2 Multi-wavelength lidar data and MODTRAN3 code

The block diagram of our multi-wavelength lidar system is shown in Fig.1. The 1064, 532, and 355 nm wavelengths are generated by a single Nd:YAG laser, and the 756 nm wavelength by a Ti-sapphire laser pumped by another Nd:YAG laser. The total energy of the output pulses is about 1.2 J with the repetition rate of 10 Hz. The back-scattered light is collected by a Newtonian telescope with 0.47 m^2 effective mirror area. Photomultipliers are used for 756, 532, and 355 nm and an avalanche photodiode for 1064 nm. The sampling rate of the time-of-flight signals is 50 MHz, which corresponds to a spatial resolution of 3 m. The resulting aerosol extinction profiles are applied to the atmospheric correction of satellite data.

An example of such profiles is exhibited in Fig.2. These data were collected on June 27, 1997 during the overflight of NOAA-14. The lidar signal (so-called A scope) for each wavelength is analyzed up to the altitude of 4 km using the Fernald method. The lidar parameter, defined as the ratio between the aerosol extinction coefficient and its back-scattering coefficient, is assumed to be 30 sr^{-1} for all the three wavelengths. The extinction coefficient profile at 550 nm is interpolated from other three profiles, which is then incorporated into the MODTRAN3 code to calculate the radiation transmission.

In MODTRAN3, there is an option of the user-defined aerosol profile where up to 34 layers can be

arbitrarily assigned. In the present case we assume 26 layers between 0 to 4 km, keeping the upper 8 layers between 5 and 100 km same as the standard model (urban aerosol, spring-summer). This profile yields the optical thickness and radiances used in the atmospheric correction on the basis of the lidar data.

In the calculation based on the standard aerosol profile, the value of the ground visibility is adjusted to obtain the same optical thickness as the lidar case for each channel (No. 1 and 2) of NOAA AVHRR. The resulting effect of atmospheric correction is compared with that of the lidar-based correction.

3 Atmospheric correction

The equations of atmospheric correction[1] employed here are as follow:

$$\rho^{(1)} = \frac{1}{a_0}\left[\frac{\pi d^2}{E_s(\lambda_i)\cos\theta_s}\{c_0(i)+c_1(i)\times DN\} - a_0\right], \quad (1)$$

$$a_0 = \frac{\pi d^2}{\cos\theta_s}\frac{\int_{\lambda_1}^{\lambda_2} L_0(\lambda)\Phi(\lambda)d\lambda}{\int_{\lambda_1}^{\lambda_2} E_s(\lambda)\Phi(\lambda)d\lambda}, \quad (2)$$

$$a_1 = \frac{d^2}{\cos\theta_s}\frac{\int_{\lambda_1}^{\lambda_2} E_g[\tau_{dir}(\lambda)+\tau_{dif}(\lambda)]\Phi(\lambda)d\lambda}{\int_{\lambda_1}^{\lambda_2} E_s(\lambda)\Phi(\lambda)d\lambda}, \quad (3)$$

$$\rho^{(2)} = \rho^{(1)} + q(\rho^{(1)} - \bar{\rho}^{(1)}), \quad (4)$$

$$q = \int_{\lambda_2}^{\lambda_1} \frac{\tau_{dif}(\lambda)}{\tau_{dir}(\lambda)}\Phi(\lambda)d\lambda, \quad (5)$$

and

$$\bar{\rho}^{(1)} = \frac{1}{N^2}\sum_{j=1}^{N^2}\rho_j^{(1)}. \quad (6)$$

In eq.(1), $\{c_0(i)+c_1(i)\times DN\}$ is the radiance received by the satellite sensor, $\Phi(\lambda)$ the sensor response function, $\tau_{dir}(\lambda)$ and $\tau_{dif}(\lambda)$ the direct and diffusive transmittance from the ground to the sensor, respectively, E_s and E_g the extraterrestrial and ground irradiance, respectively, d the Earth-Sun distance in astronomical units, θ_s solar zenith angle, $\rho^{(1)}$ the surface albedo derived from this first-step calculation, q the measure of the strength of the adjacency effect, $\bar{\rho}^{(1)}$ the average reflectance in an $N \times N$ pixel window centered on the considered pixel, and $\rho^{(2)}$ the surface albedo after the correction of adjacency effect.

If, for simplicity, the response function $\Phi(\lambda)$ is assumed to be constant, these equations are reduced into

$$\rho^{(1)} = \rho\frac{L_{pix}-L_0}{L_{tot}-L_0}, \quad (7)$$

$$\rho^{(2)} = \rho^{(1)} + \frac{L_p - L_0}{L_g}(\rho^{(1)} - \bar{\rho}^{(1)}), \quad (8)$$

where L_{pix}, L_0, L_{tot}, L_p and L_g are the radiance of the pixel, path radiance for the dark ground ($\rho = 0$), total radiance, path radiance for the atmosphere, and directly transmitted radiance after the reflection at the ground. These radiances are calculated using MODTRAN3 with an appropriate ground surface albedo of ρ (~ 0.2). In eq.(7), $(L_{tot} - L_0)$ consists of the direct and diffusive radiance reflected at the ground. In Fig.3, the albedo dependence of each radiance component calculated with the lidar-derived data is shown. One can see that $(L_{tot} - L_0)$ is proportional to ρ, so that this assumption of $\rho = 0.2$ does not affect the resulting albedo in eq.(1).

From the images of NOAA-14 AVHRR channel 1 and 2, we have selected 140 × 140 pixels including Chiba Prefecture as a test area. For the adjacency area in eq.(6) we have put $N = 3$ in the present example, which is an area of about 3 × 3 km^2.

4 Results

Each radiance component of L_0, L_p and L_g is calculated with MODTRAN3 using lidar-derived and standard atmospheric model data. The results show that among the radiance components, the multiple

[1] Richter, R., A fast atmospheric correction algorithm applied to Landsat TM images, Int. J. Remote Sensing, 1990, 11(1), pp.159–166.

scattering component, the ground reflected radiance L_g, and the dark-target path radiance L_0 are similar for both correction schemes. On the contrary there is a small difference for the atmospheric path radiance L_p, which is due to the diffusive scattering. As shown in Fig.4, the difference of L_p between the two schemes depends on the number of streams assumed in the calculation.

The images of raw data, the albedo after the first step correction, and that after the adjacency effect correction are compared in Fig.5 for NOAA AVHRR channel 1. For both the images corrected with standard atmospheric model and with lidar-derived data, there are clear differences between raw data (no correction) and corrected data ($\rho^{(1)}$ and $\rho^{(2)}$). Although the difference between the two correction schemes is small, Fig.6 shows that the aerosol profile affects the result through the adjacency effect.

5 Summary

The Atmospheric Data Correction Lidar (ADCL) is used to obtain the vertical aerosol extinction profile during the satellite overflight. The lidar-derived data and standard atmospheric data are compared in the correction of the NOAA AVHRR image.

The MODTRAN3 code is employed to calculate the radiance components using the lidar-derived and standard-model profiles. Both profiles yield similar results, yet some difference is detectable in the adjacency effect, which is related to the path radiance from the atmosphere.

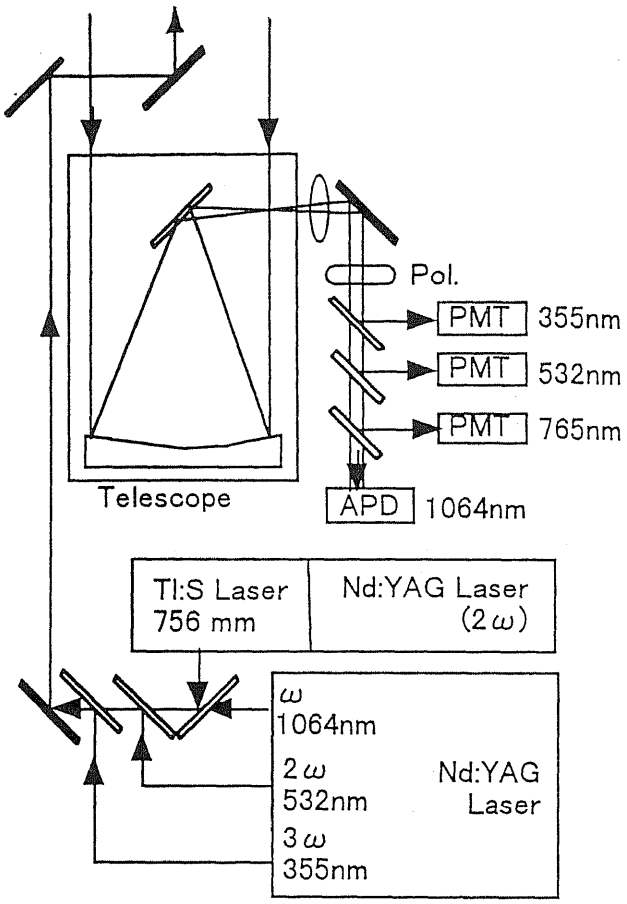

Fig.1 Block diagram of multi-wavelength lidar system

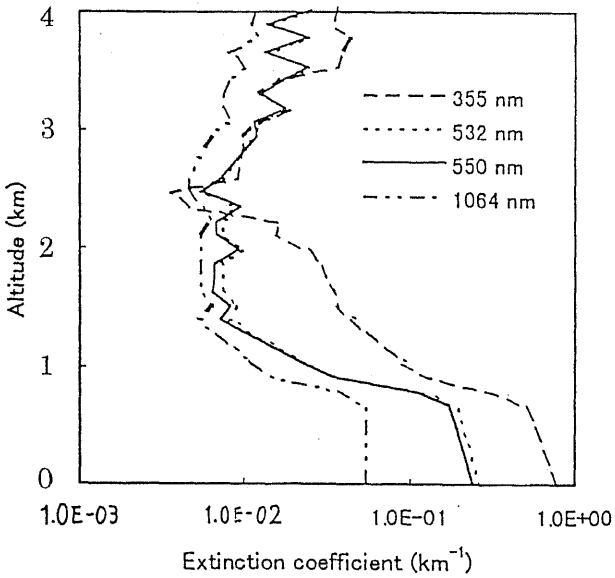

Fig.2 Vertical profiles of extinction coefficient derived from multi-wavelength lidar on June 27, 1997. The profile of 550 nm is interpolated from other three wavelengths.

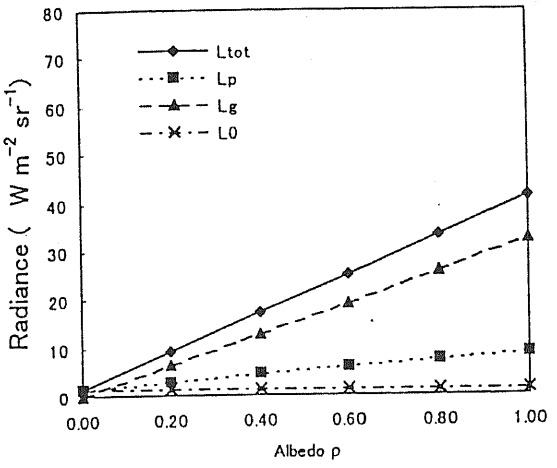

Fig.3 Albedo dependence of each radiance component, NOAA AVHRR channel 1.

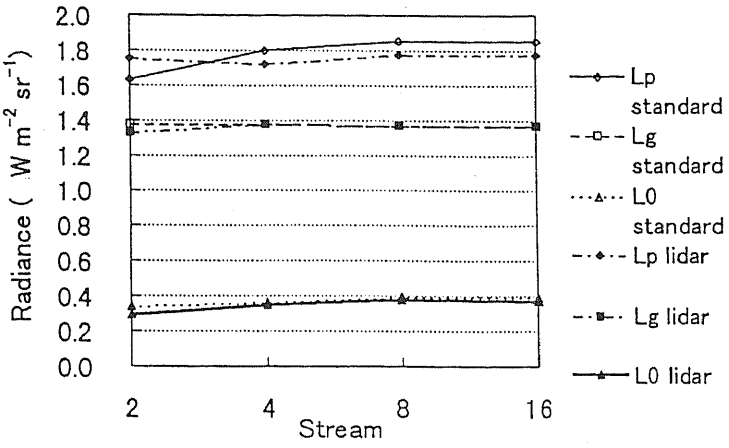

Fig.4 Multiple scattering component for each correction, NOAA AVHRR channel 1. The abscissa is the number of streams, a parameter related to multiple scattering in the MODTRAN3 code.

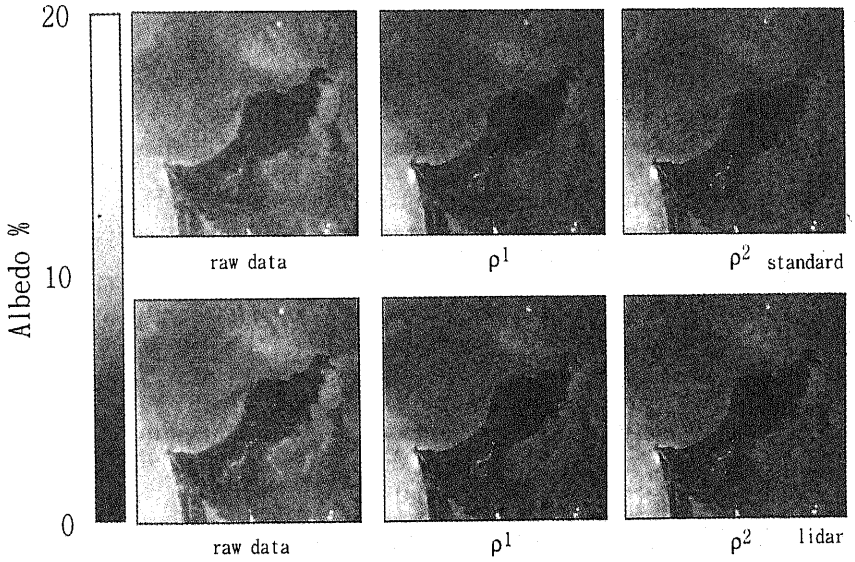

Fig.5 Atmospheric correction for standard atmospheric model and lidar-derived data, channel 1, 27 June 1997, 4 stream.

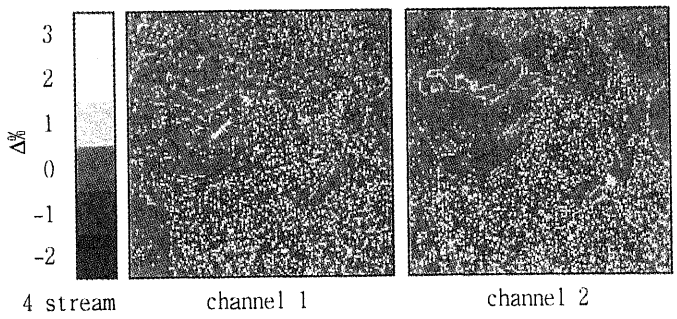

Fig.6 Difference of $\rho^{(2)}$ between the results with standard atmospheric model and lidar-derived data, ratio to the original digital numbers in percent.